

AD-A024 649

RIA-76-U304

AD

A024649

FA-TR-75069

USADACS Technical Library



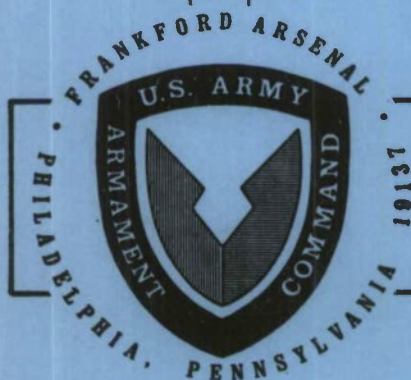
5 0712 01014345 0

TECHNICAL
LIBRARY

ION BEAM SPUTTERING OF INFRARED OPTICAL MATERIALS

August 1975

Approved for public release; distribution unlimited.



Fire Control Development & Engineering Directorate

U.S. ARMY ARMAMENT COMMAND
FRANKFORD ARSENAL
PHILADELPHIA, PENNSYLVANIA 19137

BEST AVAILABLE COPY

DISPOSITION INSTRUCTIONS

Destroy this report when it is no longer needed. Do not return it to the originator.

The findings in this report are not to be construed as an official Department of the Army position unless so designated by other authorized documents.

UNCLASSIFIED

SECURITY CLASSIFICATION OF THIS PAGE (When Data Entered)

REPORT DOCUMENTATION PAGE		READ INSTRUCTIONS BEFORE COMPLETING FORM
1. REPORT NUMBER FA-TR-75069	2. GOVT ACCESSION NO.	3. RECIPIENT'S CATALOG NUMBER
4. TITLE (and Subtitle) ION BEAM SPUTTERING OF INFRARED OPTICAL MATERIALS		5. TYPE OF REPORT & PERIOD COVERED Technical Research Report
		6. PERFORMING ORG. REPORT NUMBER
7. AUTHOR(s) J. D. LESTER H. GELLES C. BIANCHI		8. CONTRACT OR GRANT NUMBER(s)
9. PERFORMING ORGANIZATION NAME AND ADDRESS Frankford Arsenal Attn: SARFA-FCD-M Philadelphia, PA 19137		10. PROGRAM ELEMENT, PROJECT, TASK AREA & WORK UNIT NUMBERS AMCMS Code: 1497.06.7334.02 DA Project: 6747334
11. CONTROLLING OFFICE NAME AND ADDRESS U. S. Army Armament Command		12. REPORT DATE August 1975
		13. NUMBER OF PAGES 30
14. MONITORING AGENCY NAME & ADDRESS (if different from Controlling Office)		15. SECURITY CLASS. (of this report) UNCLASSIFIED
		15a. DECLASSIFICATION/DOWNGRADING SCHEDULE N/A
16. DISTRIBUTION STATEMENT (of this Report) Approved for public release; distribution unlimited.		
17. DISTRIBUTION STATEMENT (of the abstract entered in Block 20, if different from Report)		
18. SUPPLEMENTARY NOTES The authors wish to gratefully acknowledge the cooperation and assistance of John J. Walls, Jr. and Richard McKyton in the preparation of many thin films and Lawrence H. Sharper and Nathaniel Scott, Jr. for their support and encouragement. This paper was prepared with the invaluable assistance		
19. KEY WORDS (Continue on reverse side if necessary and identify by block number) Optical Materials Surface Roughness Ion Bombardment Sputtering Optical Components Infrared Optics Ion Beam Superpolishing Solid Surfaces		
20. ABSTRACT (Continue on reverse side if necessary and identify by block number) The sputter yield and morphological characteristics of materials commonly employed for infrared optical elements is described. A method to utilize a numerically controlled low energy ion beam to figure and polish infrared optical elements is presented. This method is capable of forming highly accurate large aperture optical elements without degrading optical performance by the introduction of trace impurities.		

UNCLASSIFIED

SECURITY CLASSIFICATION OF THIS PAGE(When Data Entered)

18. SUPPLEMENTARY NOTES (Cont'd)

of Mary Ann C. Urbanski. This report is based on work performed under the PEMA Program sponsored by the United States Army Armament Command.

SECURITY CLASSIFICATION OF THIS PAGE(When Data Entered)

TABLE OF CONTENTS

	<u>Page</u>
INTRODUCTION	3
OPTICAL MATERIALS	3
THE ION BEAM SPUTTERING PROCESS	3
SURFACE MORPHOLOGY INSTRUMENTATION	7
SCATTERING	7
INTERFEROMETRY	8
FECO INTERFEROMETRY	13
DIFFERENTIAL INTERFERENCE CONTRAST MICROSCOPY	13
EXPERIMENTAL INVESTIGATION	15
SPUTTER YIELD	18
SURFACE PREPARATION	21
CRYSTALLINE/POLYCRYSTALLINE	22
THE FABRICATION PROCESS	22
SYSTEM HARDWARE	25
CONCLUSIONS	25
REFERENCES	27
DISTRIBUTION	29

LIST OF ILLUSTRATIONS

Figure

1. Polycrystalline Zinc Selenide
Before Sputtering (Magnification 680 X) 5
2. Polycrystalline Zinc Selenide
Before Sputtering (Magnification 80 X) 5

LIST OF ILLUSTRATIONS (Cont'd)

<u>Figure</u>		<u>Page</u>
3.	Polycrystalline Germanium After Grazing Angle Sputtering	6
4.	Polycrystalline Germanium After Normal Incidence Sputtering	6
5.	Interferometer	9
6.	Interferometer	11
7.	Optical Heterodyne Interferometer	12
8.	FECO Interferometer	14
9.	Bi-directional Scatter Instrument	16
10.	Bi-directional Scatter Instrument	17
11.	Bi-directional Scatter Instrument	17
12.	IR Optical Element Fabrication	24
13.	Schematic, Low Energy Ion Beam Accelerator	26
14.	Low Energy Ion Beam Accelerator	26

LIST OF TABLES

<u>Table</u>	
1.	Sputter Yield of Infrared Materials 20

INTRODUCTION

A technique to shape surfaces to ultra precise contours by using a computer controlled low energy ion beam has been developed at Frankford Arsenal to produce high quality optical elements.¹ This process is presently limited to amorphous materials such as the common optical glasses. This report provides a technical foundation for increasing the capabilities of the ion beam optical fabrication process to include crystalline and polycrystalline materials as well as amorphous materials.

OPTICAL MATERIALS

Visible light refractive optical elements are commonly fabricated from materials which are amorphous. An amorphous material is one in which the atoms composing the material are randomly situated in space. This random ordering of atoms contributes very strongly to the physical properties of the material, in particular the surface roughness achievable using either conventional or ion beam polishing techniques. Glasses are generally limited to transmissions wavelengths of 6 micrometers or less. Infrared refractive optics are formed using crystalline or polycrystalline materials almost exclusively. Crystalline materials are constructed by a periodic array of atoms. Momentum is propagated in a crystal by means of quantized elastic lattice vibrations called phonons. Any deviation in a crystal from a perfect periodic array of atoms is called a crystalline defect. Common point defects are chemical inhomogenities, vacant lattice sites and interstitial atoms. Dislocations occur in crystals during crystal growth and as a response to mechanical forces on the crystal.

Crystals also exhibit plastic properties which are irreversible deformations such as yield and slip. We are also directly concerned with reversible elastic properties of crystals. These properties effect the sputter yield parameters and directly influence the surface micro-structure resulting from ion bombardment of the surface.

THE ION BEAM SPUTTERING PROCESS

As an energetic ion approaches a solid surface there is a very high probability that the ion will be neutralized by capturing an electron. The mechanism of interest in the ion beam process therefore, is one of an atom with large translational kinetic energy interacting with relatively fixed atoms which form the surface and near surface of a solid. At the relatively low energies employed in the figuring and polishing process the interactions are characterized by elastic nuclear collisions and inelastic electronic excitations. Atoms are removed from solid surfaces as the result of a momentum transfer from the incident atom to atoms of the target solid. This process is called sputtering.

¹ J. D. Lester, Forming Precision Optics Using an Ion Beam, Frankford Arsenal Report R-2087, (1973).

A single incident ion typically will directly interact with several target atoms. Because of the coupling forces among atoms comprising the target solid, many atoms not directly involved in collisions with the incident atom will experience a transfer of momentum from the initial interactions. The differences in response to ion beam sputtering exhibited by crystalline/polycrystalline materials as distinguished from amorphous materials is due in large part to the efficient momentum transfer mechanism in crystals. This efficient propagation of momentum (phonons) away from the locus of the initial ion target atom collision is due to the ordered periodic placement of atoms in the target. In contrast with amorphous materials in which the atoms are randomly situated and momentum waves damped out within a short distance of the primary interaction, the periodic nature of a crystal effectively propagates the momentum transferred from the incident ion large distances away from the region of impact of the ion on the surface. The momentum wave is typically terminated at a crystalline defect. If the crystalline defect is on the surface or near surface region of the solid, sufficient momentum may be imparted to one or more atoms to cause the atoms to be removed from the solid. Figures 1 and 2 illustrate this effect on a macroscopic scale. Figure 1 is a photomicrograph of zinc selenide (ZnSe) showing the polished polycrystalline surface before ion beam sputtering. Figure 2 is a photomicrograph of the same surface after radiation by approximately 10^{17} ions/cm² singly ionized argon at a kinetic energy of 35×10^3 electron volts. The resultant surface has been highly decorated by the sputtering action of the ions. The grain boundaries of the crystallinities are surface crystalline defects, hence the momentum transfer mechanism has caused a substantial number of atoms located at the grain boundaries to be removed from the surface; resulting in the decoration shown.

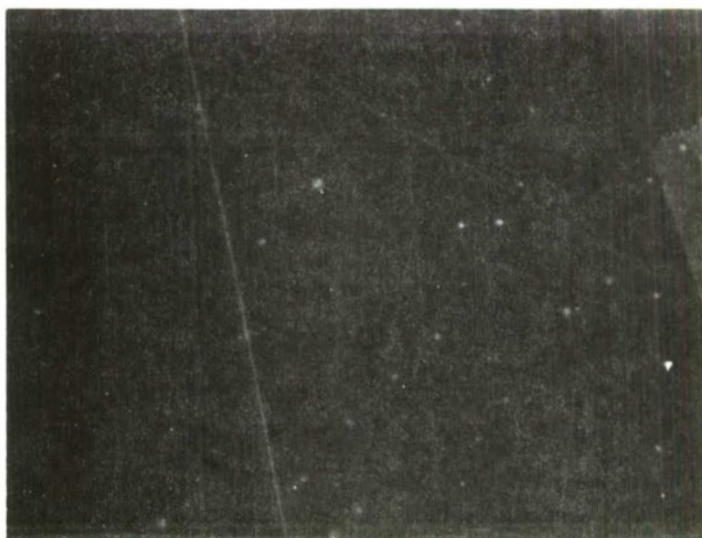
Ion beam induced sputtering of solids which are composed of ordered arrays of atoms is strongly influenced by the relative geometries of the ion beam and the atoms of the solid. Figures 3 and 4 show the effect of sputtering a polycrystalline surface with an ion beam incident in one case near grazing angle, and in the other, normal. The photomicrograph shown in Figure 3 exhibits a characteristic terrace-shoulder pattern. This is typical of polycrystalline materials sputtered by an ion beam incident at near grazing angle. Figure 4 shows the result of sputtering the same polycrystalline material at an angle normal to the surface. The hemispherical patterns are typical both of normal attack angle ion sputtering and also chemical etch.

Similar results have been reported in the literature for many other crystalline materials such as copper², gold, zinc, aluminum³ and silver⁴.

² G. D. Magnuson, B. Meckel and P. Harkins, J. Appl. Phys. 32, 369 (1961).

³ R. Cunningham et al, J. Appl. Phys. 31, 839 (1960).

⁴ G. Wehner, Phys. Rev. 102, 690 (1956).



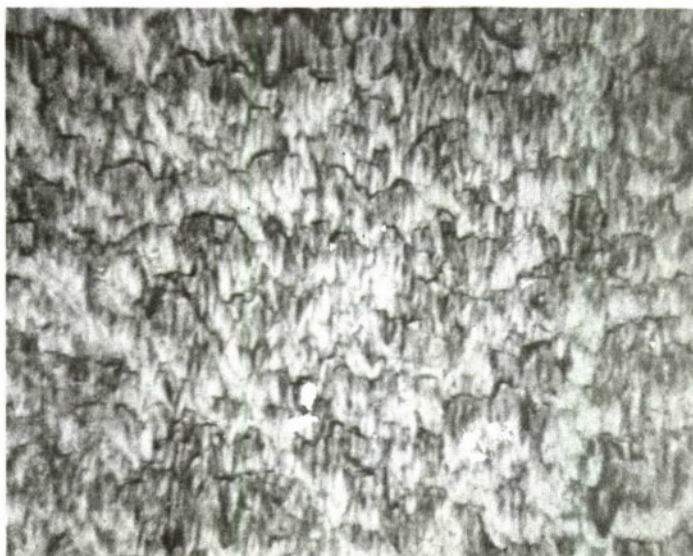
Magnification 680 X

Figure 1. Polycrystalline Zinc Selenide Before Sputtering



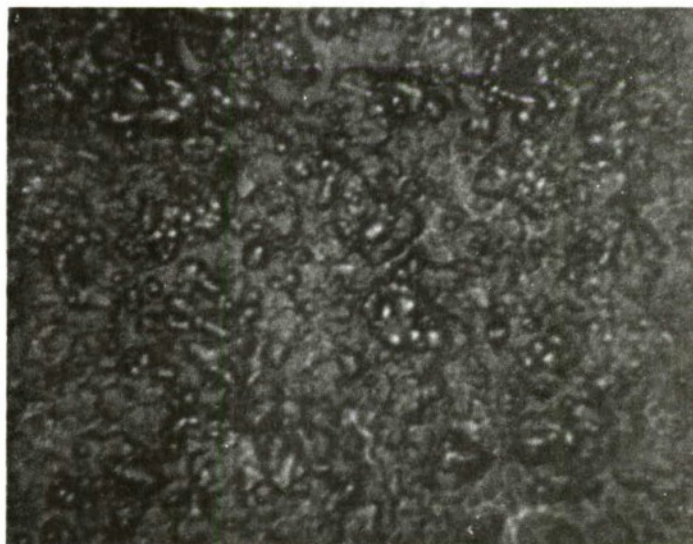
Magnification 80 X

Figure 2. Polycrystalline Zinc Selenide After Sputtering



Magnification 680 X

Figure 3. Polycrystalline Germanium After Grazing Angle Sputtering



Magnification 680 X

Figure 4. Polycrystalline Germanium After Normal Incidence Sputtering

Many theories^{5,6,7,8,9} have been advanced which try to describe the sputtering events in crystalline materials. Most of these are empirical with little or no attempt to relate to the complex interactions which must occur in the crystal. Many theories are currently being developed; these are well described in reference 10. One of the most successful theories which is somewhat more rigorous and physical than most is due to Martynenko^{11,12}. This theory takes focused collision chains into account. A fairly good fit to experimental data has been achieved.

SURFACE MORPHOLOGY INSTRUMENTATION

As described above, infrared optical materials because they are crystalline have a tendency to develop microscopic patterns on the surface while being eroded by an ion beam. It is important then, that in addition to measuring the surface figure and optical transmission characteristics of an infrared optical element that the surface roughness be measured. Several schemes are available which have enough resolution for this task. The most promising techniques will be described.

SCATTERING

H. E. Bennett and his co-workers have been very active in the relation of scattering theory to surface roughness. Bennett has developed expressions which relate the specular reflectance of plane surfaces to the microscopic roughness of the surface¹³.

⁵ E. Lamar and K. Compton, Science 80, 541 (1934).

⁶ D. T. Goldman and A. Simon, Phys. Rev. 111, 383 (1958).

⁷ E. Henschke, Phys. Rev. 121, 1286 (1961).

⁸ E. Langberg, Thesis Dept. Elect. Eng., Princeton Univ. (1956).

⁹ P. Rol, J. Fluit, and J. Kistemaker, Physica 26, 1009 (1960).

¹⁰ Yu. V. Martynenko, Soviet Phys. Sol. State 6, 1581 (1965).

¹¹ Yu. V. Martynenko, Soviet Phys. Sol. State 6, 2827 (1965).

¹² G. Carter and J. Colligon, Ion Bombardment of Solids, New York, American Elsevier Publishing Company, 1968.

¹³ H. E. Bennett and J. O. Porteus, J. Opt. Sol. Am, 51, 123 (1961).

Bennett develops expressions which relates the reflection of a parallel beam of monochromatic light from a rough metal surface to the reflection from a standard surface of the same material. The expression cited by Bennett for specular reflection at normal incidence is

$$R_S = R_O e^{-(4\pi\sigma)^2/\lambda^2} \quad (1)$$

where: σ is root mean square surface roughness
 λ is wavelength
 R_O is specular reflectance of standard surface
 R_S is specular reflectance of test surface

If the diffusely reflected light is measured with an instrument with an acceptance angle $\Delta\theta$ the complete expression for the measured reflectance is

$$R = R_O e^{-(4\pi\sigma)^2/\lambda^2} + R_O \frac{32\pi^4}{m^2} \left(\frac{\sigma}{\lambda}\right)^4 (\Delta\theta)^2 \quad (2)$$

where m^2 is mean square slope

This relationship is independent of the slope of the surface if measurements are made at sufficiently long wavelength. If the wavelength is large in comparison with the dimensions of the surface roughness the quantity $(\sigma/\lambda)^4$ becomes negligible and thus σ^2 is directly proportional to the quantity $\ln(R_O/R)$. The primary disadvantage of this method is that since the measurement is relative, well defined surface standards must be provided for each material of interest. In addition, these standards must be cross-referenced to some primary roughness standard.

INTERFEROMETRY

Several methods of measuring surface roughness using interferometric techniques have appeared in the literature. Ribbens¹⁴ proposed the system shown in Figure 5. In this scheme the surface roughness is related to the contrast ratio of the fringes. While this method is capable of resolving roughness of the order of approximately 1 nanometer (10 Angstroms) RMS, care must be taken to obtain the highest possible laser monochromaticity. Obviously, the surface of the reference mirror must be smoother than the sample

¹⁴ W. B. Ribbens, Appl. Optics 8, 2173 (1969).

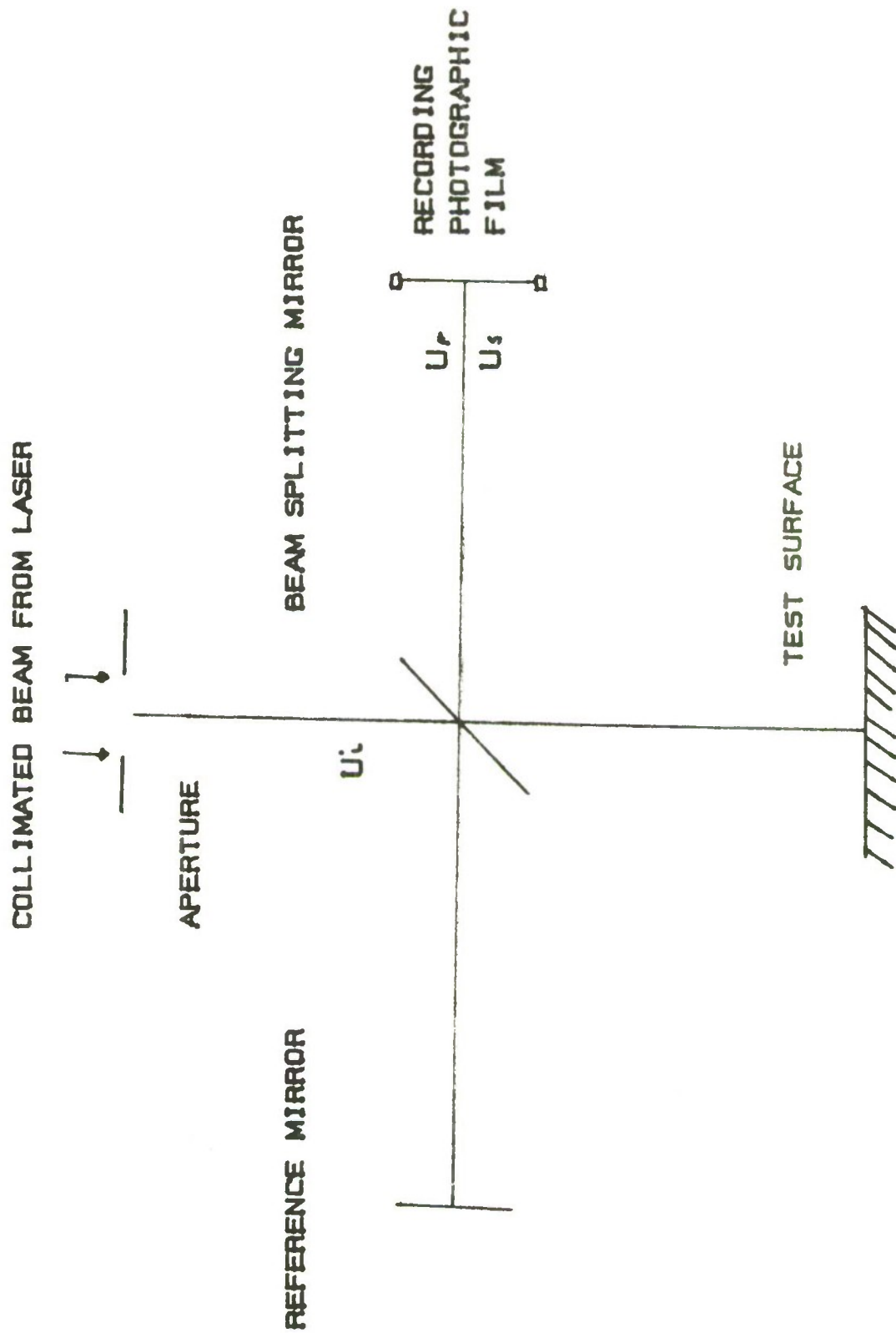


Figure 5. Interferometer (See Ref. 14)

being tested. Ribben's expression relating surface roughness to fringe contrast is:

$$\sigma = \frac{\lambda}{4\pi} \ln \left(\frac{(R+1)^{\frac{1}{2}}}{\rho(R-1)^{\frac{1}{2}}} \right) \quad (3)$$

where ρ is ratio of reflectivities of the reference and test surfaces
 R is the fringe contrast ratio

A different interferometric technique which does not require a reference surface as a standard was outlined by Motycka¹⁵. This method uses a Jamin interferometer to form pairs of coherent beams which are reflected from the test surface and caused to interfere. Figure 6 shows the arrangement of this system, Motycka defines a quantity which he calls the fringe visibility V with the following equation:

$$V = \frac{J_{\max} - J_{\min}}{J_{\max} + J_{\min}} \quad (4)$$

Motycka then develops this final equation relating the RMS roughness to the fringe visibility:

$$V(\mu) = \left[1 - 1 - \gamma(\mu) \right] \left(\frac{2}{2!} \chi^2 \sigma^2 - \frac{2}{4!} \chi^4 \sigma^4 + \frac{2^5}{6!} \chi^6 \sigma^6 - \dots \right) \quad (5)$$

where μ is the lateral shear
and $\gamma(\mu)$ is the autocorrelation function.

An optical heterodyne interferometer has been adapted by Hildebrand¹⁶ to provide surface roughness measurements. Figure 7 shows the system. A Bragg cell modulates a laser beam to form two separate beams, one at the laser frequency the other with the sum of the laser frequency and the modulation frequency. One beam is focused on the test surface; the other directly on a detector. The light reflected by the test surface is collected and also focused on the detector. The detector will respond to the beat frequency of the two incident light beams. If the test sample is translated under the beam, surface roughness will induce a doppler shift in frequency of the reflected beam proportional to the profile of the surface. The amplitude of the photodetector output is proportional to the depth of the roughness and the frequency of the

¹⁵ J. Motycka, Appl. Optics 8, 1435 (1969).

¹⁶ B. Hildebrand "Surface Roughness Measurements by an Optical Heterodyne Technique," IMOG Subgroup on Gaging, 33rd Meeting (1972).

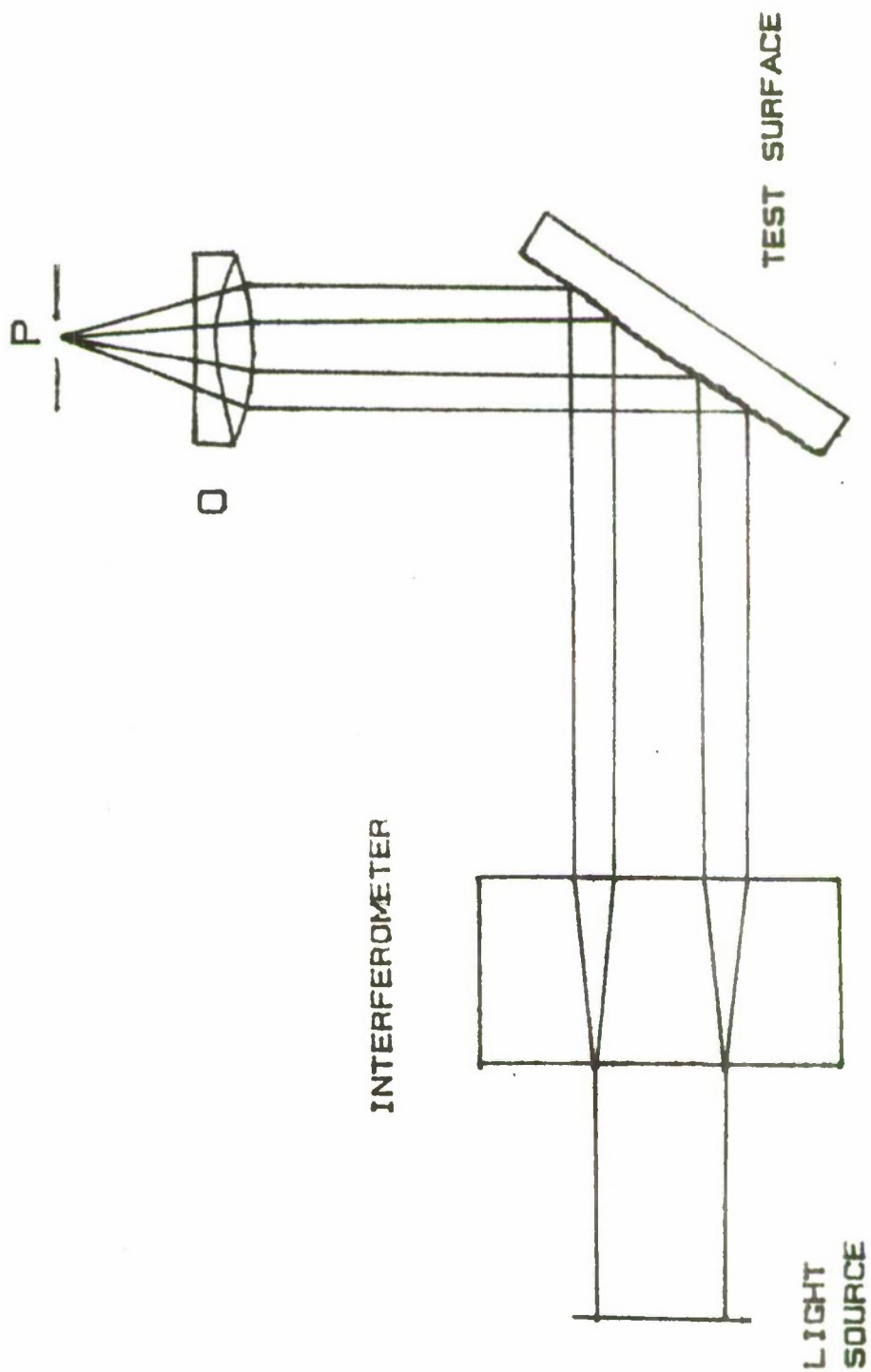


Figure 6. Interferometer (See Ref. 15)

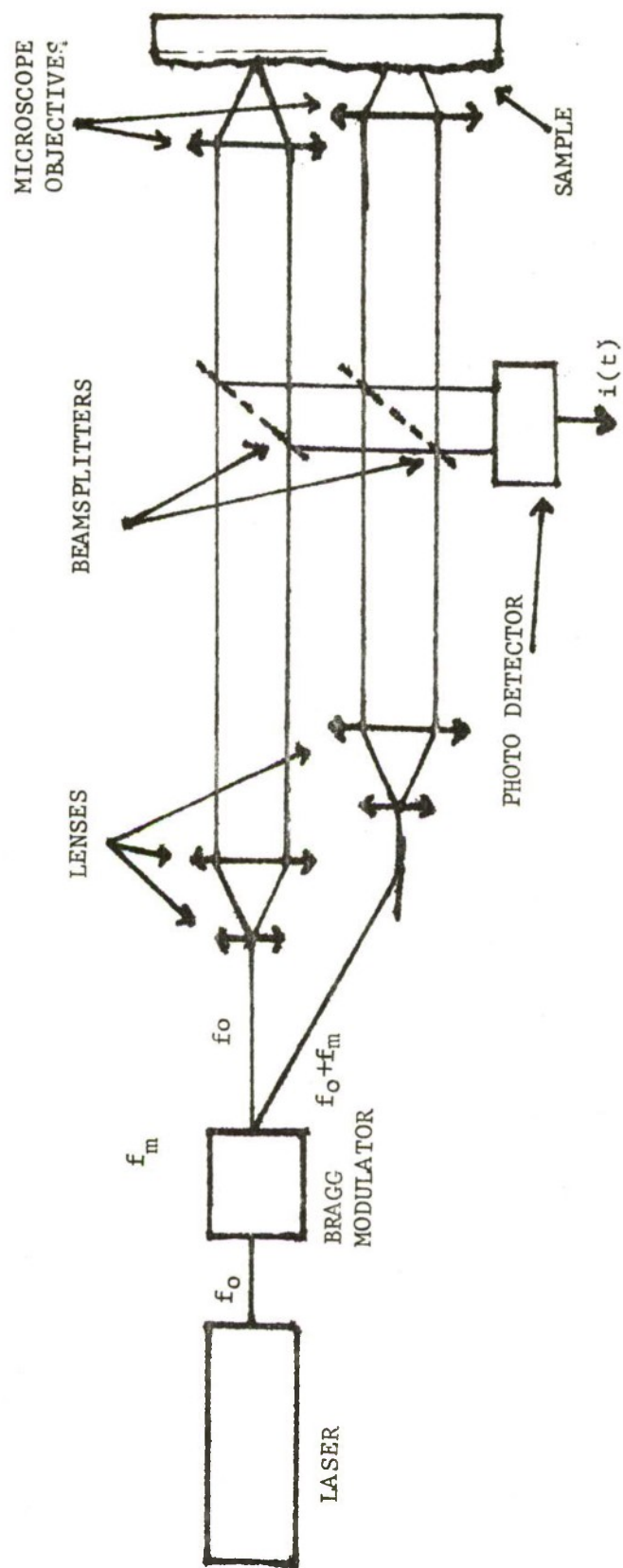


Figure 7. Optical Heterodyne Interferometer (See Ref. 16)

output, when related to the translation velocity, provides the autocorrelation data. This system is capable of tracing the profile of a rough surface with a resolution of 1 nanometer normal to the surface.

FECO INTERFEROMETRY

J. M. Bennett¹⁷ has developed an instrument which employs multiple beam fringes of equal chromatic order to measure surface roughness on polished optical flats. The test surface is combined with a partially silvered optical flat to form an interferometer. The silvered flat must be as smooth as possible. The Feco Interferometer is shown in Figure 8. The test surface is illuminated with white light and the output of the Interferometer is dispersed by a spectrograph. The equal chromatic order fringes which profile the surface of the flats provide a direct measure of the peak to peak surface roughness¹⁸. J. Bennett develops the following relationships:

$$\sigma_{p-p} = \frac{\lambda_1 (\Delta\lambda)}{2(\lambda_1 - \lambda)} \quad (6)$$

where λ_1 is the wavelength of fringe being measured
 λ is wavelength of adjacent fringe

If a Gaussian distribution of height is assumed:

$$\sigma_{RMS} = \sigma_{p-p} / 2(2)^{1/2} \quad (7)$$

This system has gained the most acceptance as the instrument for quantitative measurement of surface roughness of superpolished surfaces. It is however, moderately difficult to implement and certainly provides greater resolution than required for this program.

DIFFERENTIAL INTERFERENCE CONTRAST MICROSCOPY

This is a standard metallurgical technique which is useful for observing the structure of the surface roughness but which is incapable of providing quantitative measurements. An interference contrast microscope has been assembled in the laboratory and has produced many of the photomicrographs used in this study.

¹⁷ J. M. Bennett, J. Opt. Soc. Am. 54, 612 (1964).

¹⁸ R. W. Dietz and J. M. Bennett, Appl. Optics 5, 81 (1966).

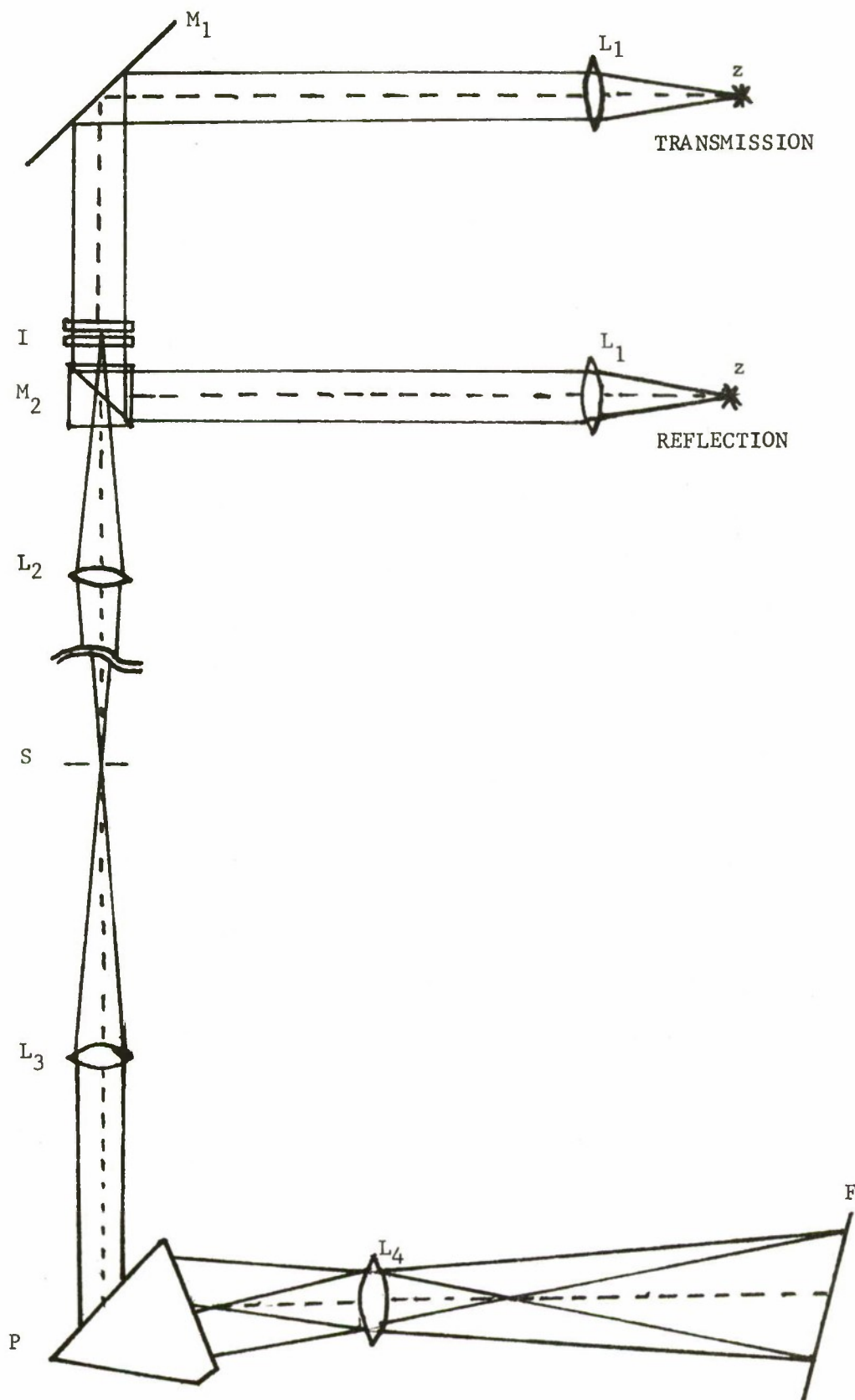


Figure 8. FECO Interferometer (See Ref. 17)

EXPERIMENTAL INVESTIGATION

Using the work of Hildebrand¹⁹ and Slomba²⁰ as a basis, a bi-directional scatter distribution instrument was assembled. This instrument is capable of measuring the angular distribution of light scattered from a surface from which the RMS surface roughness and the period and orientation of surface irregularities can be extracted. Excellent agreement with absolute measurements made by Bennett and Bennett using absolute scattered light measurements and FECO interferometry have been reported by Hildebrand. Figure 9 is a diagram showing the basic instrument. Figures 10 and 11 are photographs of the system assembled and employed in our laboratory. The photomultiplier is mounted on a milling head which is capable of accurately rotating on an arc with the test surface at the center. The output of the PMT was monitored on a plotter. The instrument is based on the equation for scattering from a rough surface with Gaussian distribution of heights developed by Bennett¹³. Bennett's equation which relates the fraction of light reflected from a test surface into an angle between θ and $\theta + \Delta\theta$ at an angle θ from the normal to the surface is modified slightly by Hildebrand to yield:

$$\omega(\theta) = \frac{I(\theta)}{I(\theta_0)} = \frac{2\pi^4 a^2 \sigma^2}{\lambda^4} (\cos \theta + 1)^4 \sin \theta \exp \left[- \frac{(\pi a \sin \theta)^2}{\lambda^4} \right] \exp \left(\frac{4\pi\sigma}{\lambda} \right)^2 \quad (8)$$

where $I(\theta)$ is irradiance at angle θ
 $I(\theta_0)$ is irradiance of the specular reflection
 a is auto covariance length of the surface
 σ is RMS surface roughness
 λ is wavelength

Hildebrand forms a ratio:

$$\Omega_n(\theta) = \frac{\omega_n(\theta)}{\omega_s(\theta)} = \left(\frac{a_n \sigma_n}{a_s \sigma_s} \right)^2 \exp \left[\left(\frac{4\pi^2}{\lambda} \right)^2 (\sigma_n^2 - \sigma_s^2) \right] \exp \left[- \left(\frac{\pi \sin \theta}{\lambda} \right) (a_n^2 - a_s^2) \right] \quad (9)$$

¹⁹ B. Hildebrand, R. Gordon and E. Allen, Appl. Optics 13, 177 (1974)

²⁰ Reported in: Microinch Machining of Optical Components for Infrared Optics by Capt. T. T. Saito, USAF, Air Force Weapons Laboratories, Rept. AFWL-TR-73-290 (1974).

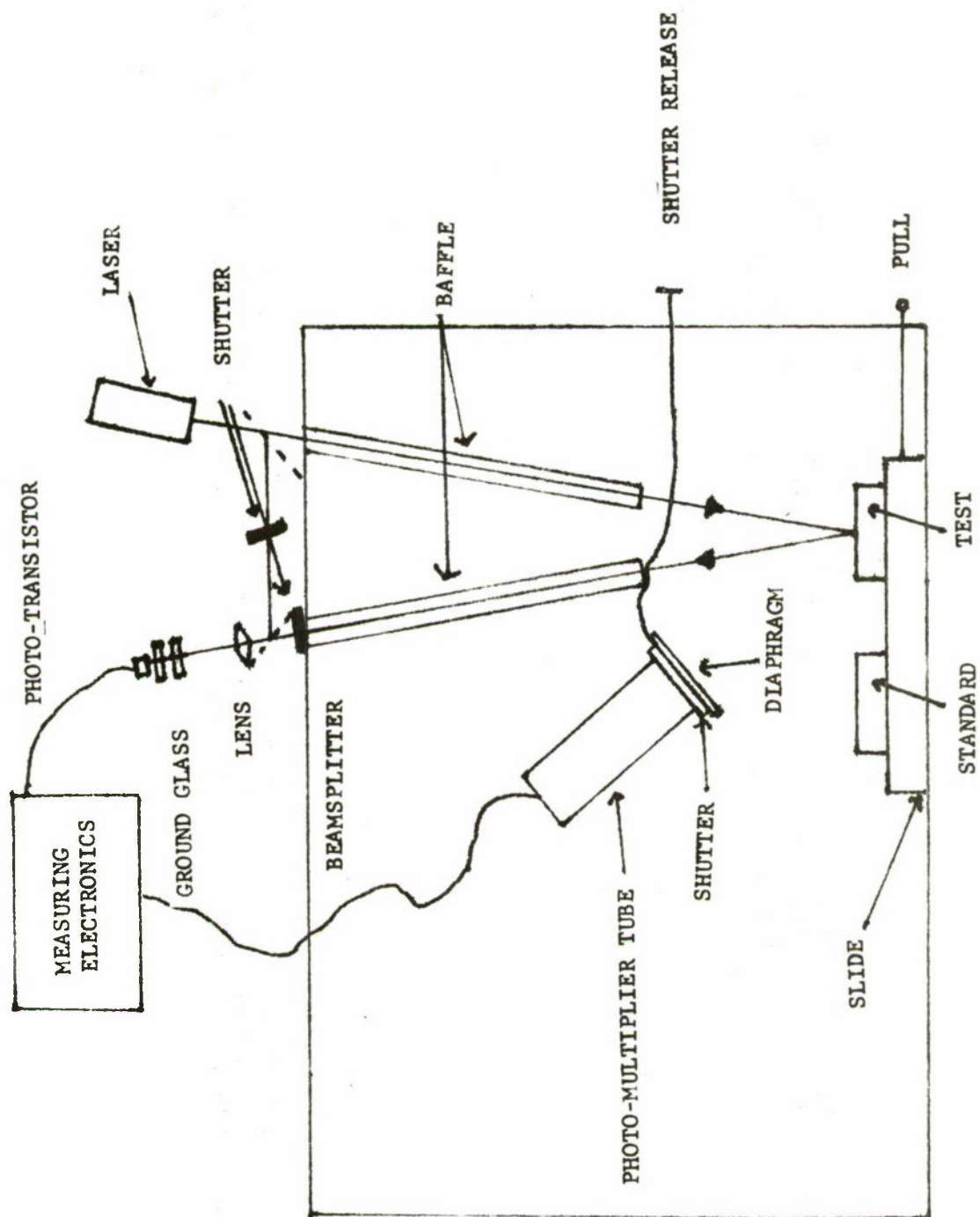


Figure 9. Bi-directional Scatter Instrument (See Ref. 19)

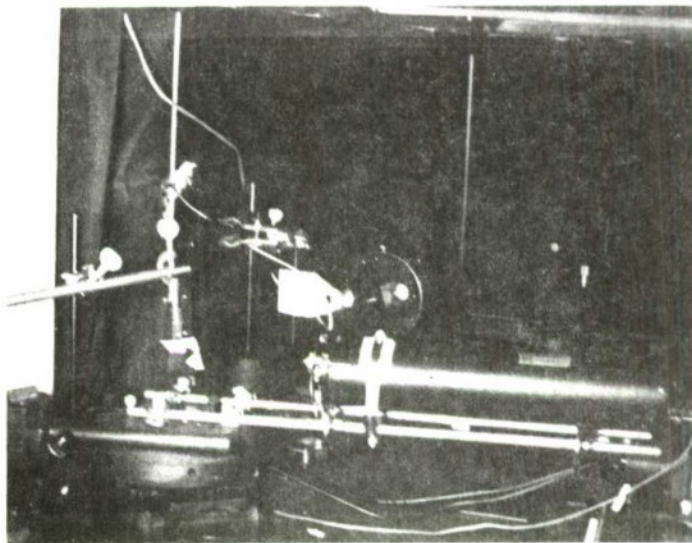


Figure 10. Bi-directional Scatter Instrument

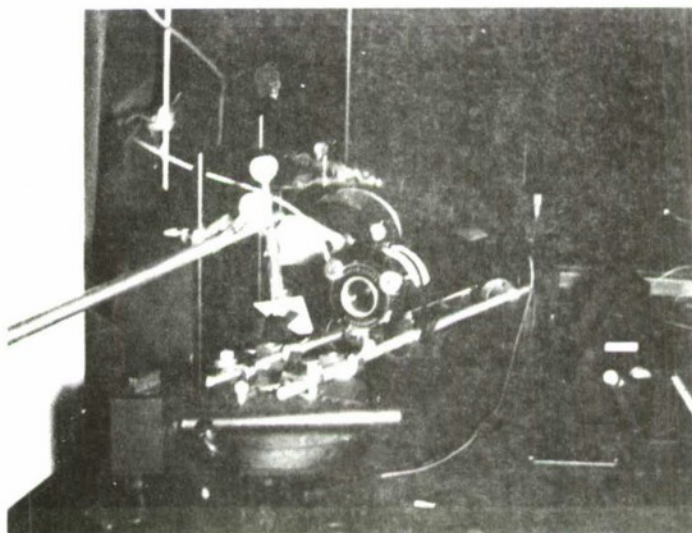


Figure 11. Bi-directional Scatter Instrument

where the subscript n labels the test surface and s the reference surface. Hildebrand simplifies equation 9 by assuming $a_n \approx a_s$ and $\sigma/\lambda \ll 1$ to obtain:

$$\sigma_n = \bar{\Omega}_n^{1/2} \sigma_s \quad (10)$$

where $\bar{\Omega}_n$ is $\Omega_n(\theta)$ averaged over a number of measurements at various angles. Using this simplification, good to excellent agreement has been achieved with the more rigorous (and more cumbersome) FECO Interferometer and absolute integrated scatter instrument. Remarkably enough, good experimental correlation has also been observed when an aluminum overcoated quartz mirror was used as the reference mirror for measurements on other materials. This is a bonus because although equations 8 and 9 are independent of reflectivity, there is no a priori justification of the simplifying assumption that the autocovariance functions are approximately equal for different materials.

This fortunate occurrence results in a considerable reduction in the requirement for accurately measured, superpolished reference mirrors. The system will be interfaced to a minicomputer which will perform all the required instrumentation control functions and data reduction functions.

SPUTTER YIELD

The major justification for employing an ion beam to shape and polish optical surfaces is the precision of the material removal of the ion beam sputtering process. Once the yield curves have been empirically established for a specific ion-target combination, the number of atoms removed from the surface of a target may be very accurately calculated as a function of such easily measured external parameters as ion species, ion kinetic energy, ion beam current and relative angle of incidence.

An important property of the sputtering process is that the chemical composition of the target is usually maintained even though the elements of the target may have considerably different sputter yields when measured on homogeneous elemental targets. Several explanations of this fortuitous effect have appeared in the literature. Maissel²¹ suggests a very thin "altered region" which becomes deficient in the higher sputtering yield elements very quickly upon initiation of the sputtering process. The relative enrichment of the lower yield components soon compensates for their lower removal rates thus maintaining the original chemical composition.

²¹ L. Maissel and R. Glang, Handbook of Thin Film Technology, McGraw-Hill, NY, NY (1970).

Some experiments conducted by Wolsky strongly suggest that molecular sputtering may occur in some cases which maintain chemical composition without the formation of the thin altered layer at the target surface.

Because chemical stoichiometry is maintained whatever the mechanism the sputter yield is typically provided in units of atoms removed per incident ion without any effort to identify or distinguish the elemental species of a multielement target. For our purposes, a somewhat more practical sputter yield coefficient is obtained by determining the volume of target material removed under our standard operating conditions per incident ion. We commonly express sputter yield in terms of nanometers of materials removed per square centimeter per unit beam current per second for a specific ion specified-target material at a given accelerating potential. This volumetric sputter yield may be determined by direct experimental measurement but the process involves an accurate measure of very small volumes and is very vulnerable to experimental error. Because the materials we have chosen to investigate have been relatively well characterized in the literature, an indirect but more accurate method of determining the sputter yield was chosen. This method entails determination of the weight loss of a sample caused by sputtering the sample under carefully controlled conditions with an accurately determined number of ions. This provides a direct measurement of the target weight loss per incident ion. Weight losses of the order of 0.5 mg to 1.0 mg were measured. The sputter yield was calculated using equation 11.

$$Y = \frac{\Delta w}{IM} \quad (11)$$

where Y is sputter yield (atoms/ion)

Δw is weight loss of target

I is total incident ions = $\int_0^t i(t)dt$

M is average atomic weight of target material

A minicomputer was used to determine the total number of incident ions. The suppressed ion beam current was monitored at intervals of a few seconds by programming the computer to deflect the ion beam onto a faraday cup. The current is measured and the total incident number of ions is calculated by integration. This is converted into volume sputter yield using crystalline structure and density. Table 1 lists the measured sputter parameters for a large number of infrared optical materials. The figures presented for polycrystalline materials are for random orientation of the crystallites. The single crystal samples were sputtered at several different orientations to provide some indication of the sputter yield dependence on relative beam lattice orientation.

Table 1. Sputter Yield of Infrared Materials

Si	(single crystal, normal incidence, 35 KeV)	Yield = 0.960 atoms/ion
Si	(single crystal, grazing angle, 45 KeV)	Yield = 1.50 atoms/ion
AgBr	(polycrystalline, normal incidence, 35 KeV)	Yield = 7.875 atoms/ion
KCl	(polycrystalline, normal incidence, 30 KeV)	Yield = 37.57 atoms/ion
NaCl	(single crystal, normal incidence, 30 KeV)	Yield = 45.30 atoms/ion
MgF ₂	(polycrystalline, normal incidence, 30 KeV)	Yield = 23.21 atoms/ion
ZnS	(polycrystalline, normal incidence, 30 KeV)	Yield = 4.26 atoms/ion
CaF ₂	(polycrystalline, normal incidence, 30 KeV)	Yield = 6.70 atoms/ion
ZnSe	(polycrystalline, normal incidence, 30 KeV)	Yield = 3.61 atoms/ion

SURFACE PREPARATION

It is essential that all crystalline infrared materials have a carefully prepared surface before the ion beam figuring and polishing process is initiated. The first step in the surface preparation process is a high density plasma etch to remove all contamination from the surface and near surface of the optical blank. This step is critical to the final optical performance of the finished element. Crystalline and polycrystalline materials are very susceptible to "loading" of impurities by diffusion and mechanical implantation. Also, in contrast with glasses employed for visible wavelength optical elements, infrared materials are chemically reactive with substances. This is a serious problem because the presence of trace amounts of contaminants, many very common, seriously degrades the infrared transmission characteristics of the material. For example, in the case of the alkali halide materials, trapping of OH radicals in the crystal through contact with water either during fabrication of the optical blank or from high atmospheric humidity leads to a significant increase in the optical absorption.^{22,23,24} The inclusion of particles of polishing compound during conventional polishing or impurity atoms or radicals present as interstitials in the near surface region will degrade the infrared performance through the formation of color centers, scattering and absorption.

Because the ion beam sputtering process completely avoids sources of contamination it is well suited for fabricating infrared optical elements. Inert gas ions are usually employed for the ion beam sputtering process. These ions are chemically inactive therefore there is no danger of formation of undesired compounds by reaction with the optical material. Much of the kinetic energy of the ions is transferred to the atomic structure of the target resulting in localized heating. This higher temperature increases the diffusion of any trapped inert gas atoms to the surface of the optical element where it escapes. The entire process takes place in a high vacuum. Once the ion beam figuring and polishing process is completed, the surface may be coated with antireflection and passivation optical coatings before exposure to the atmosphere. The ion beam optical polishing process when applied to crystalline/polycrystalline materials to fabricate infrared optical elements results in a precisely contoured, highly polished surface without contamination either on the surface or in the bulk.

-
- ²² E. Bernal et al, Preparation and Characterization of Polycrystalline Halides for Use in High Power Laser Windows, Honeywell Research Center, Rept. No. HR-74-252:5-26 ARPA Order Nos. A02172/1 and AD2416 (1974).
- ²³ L. Maissel, Loc Cit.
- ²⁴ G. Bassett Proc. European Conf. Electron Microscopy, DELFT (1960).

CRYSTALLINE/POLYCRYSTALLINE

Materials have a pronounced tendency to become decorated on the surface as a result of the complex collision and momentum transfer processes described above. In addition, sputter yield is dependent on the relative orientation of the crystal structure with respect to the incident ion beam. In most cases therefore it is necessary to alter the structure of the surface and near surface region of the optical blank before application of the ion beam sputtering process. The surface preparation procedure includes cleaning the surface and forming a region at the surface where the structure is disoriented and resembles an amorphous rather than crystalline structure. In actual practice, a stable amorphous layer may not always be possible, however, by careful application of thin film disposition procedures, a very fine grained layer may be formed which has all the necessary structural characteristics. This altered region must be thick enough to allow the ion beam to figure the desired contour on the surface without exposing the underlying crystalline material substrate. The concept of altering the surface region of a material prior to figuring and polishing is a new and unique approach recently developed in our laboratory²⁵ for ion beam superpolishing metal mirrors for high energy laser applications. A similar technique has been developed independently at Battelle Northwest Laboratories for surface preparation of metals prior to conventional polishing.²⁶ This method has proven to produce stable, extremely fine grained or amorphous layers well suited for ion beam figuring.

THE FABRICATION PROCESS

There are two important reasons for employing an ion beam to shape and polish infrared optical elements.

First, the precision of the material removal process using an ion beam permits modified open loop numerical control of the entire fabrication process. Secondly, the most infrared optical materials are chemically reactive and relatively soft thus permitting trace impurities to accumulate in the material during the conventional figuring and polishing process. In most cases these impurities seriously degrade the optical characteristics of the material. The ion beam process does not introduce any contamination.

Modern optical design practice utilizes computers to generate a mathematical description of the surface of a desired optical element. This description is usually in terms of the slope of the surface or,

²⁵ J. D. Lester and R. T. Cook, Ion Beam Superpolishing of Metal Mirrors, Proc. 1974 Frankford Arsenal Spring Technical Symposium (1974).

²⁶ M. J. Soileau et al in High Energy Laser Mirrors and Windows, H. Bennett, editor Semi-annual report No.4 ARPA Order 2175 (1974).

alternately, the heights of a matrix of elemental surface areas with respect to some reference point on the surface. To fabricate this optical element it is necessary to remove material from the optical surface in a controlled manner, using the ion beams. In general, each elemental area of surface of the solid will require the precise removal of a different amount of material.

In order to permit the amount of material removed to vary as a function of position, it is necessary to focus the ion beam to a diameter of the order of the smallest elemental area required by the mathematical description of the desired surface. The amount of material removed from a specific elemental surface is varied by controlling the total number of ions incident on that area. The ion specifies ion energy, and angle of incidence of the ion beams are held constant at the desired values during the fabrication process. The fabrication procedure proceeds as an "open loop" process in that the optical surface is not monitored during the ion beam sputtering operation. The ion beam current and deflection control is monitored by the computer at intervals of a few seconds and the sputtering process is corrected for any change in the ion beam characteristics.

Figure 12 shows the procedure used in the fabrication of precision infrared optical elements.

Step 1 - The optical designer, aided by a computer utilizing standard optical design software, generates an accurate mathematical description of a desired infrared optical element.

Step 2 (BFPSL Program) - From the mathematical description, a specially developed computer software routine (BFPLS) generates a new mathematical description of the spherical or parabolic surface which is the "best fit" to the desired surface in terms of least material removal using the ion beam sputtering process. This procedure is used solely to reduce working time in the ion beam system by performing gross shaping of the surface by conventional mechanical techniques. This step may often be avoided.

Step 3 - The preliminary optical blank is formed by cutting, grinding and rough polishing the infrared optical material to approximate the required element dimensions.

Step 4 - The preliminary optical blank is cleaned in a high vacuum using plasma induced sputtering to remove the surface layer contaminated by the initial blank preparation in step 3. An amorphous or pseudo amorphous layer is deposited.

Step 5 - The surface error matrix is developed which describes the surface using a very large number of elemental surface areas together with the quantity of material to be removed from each elemental area.

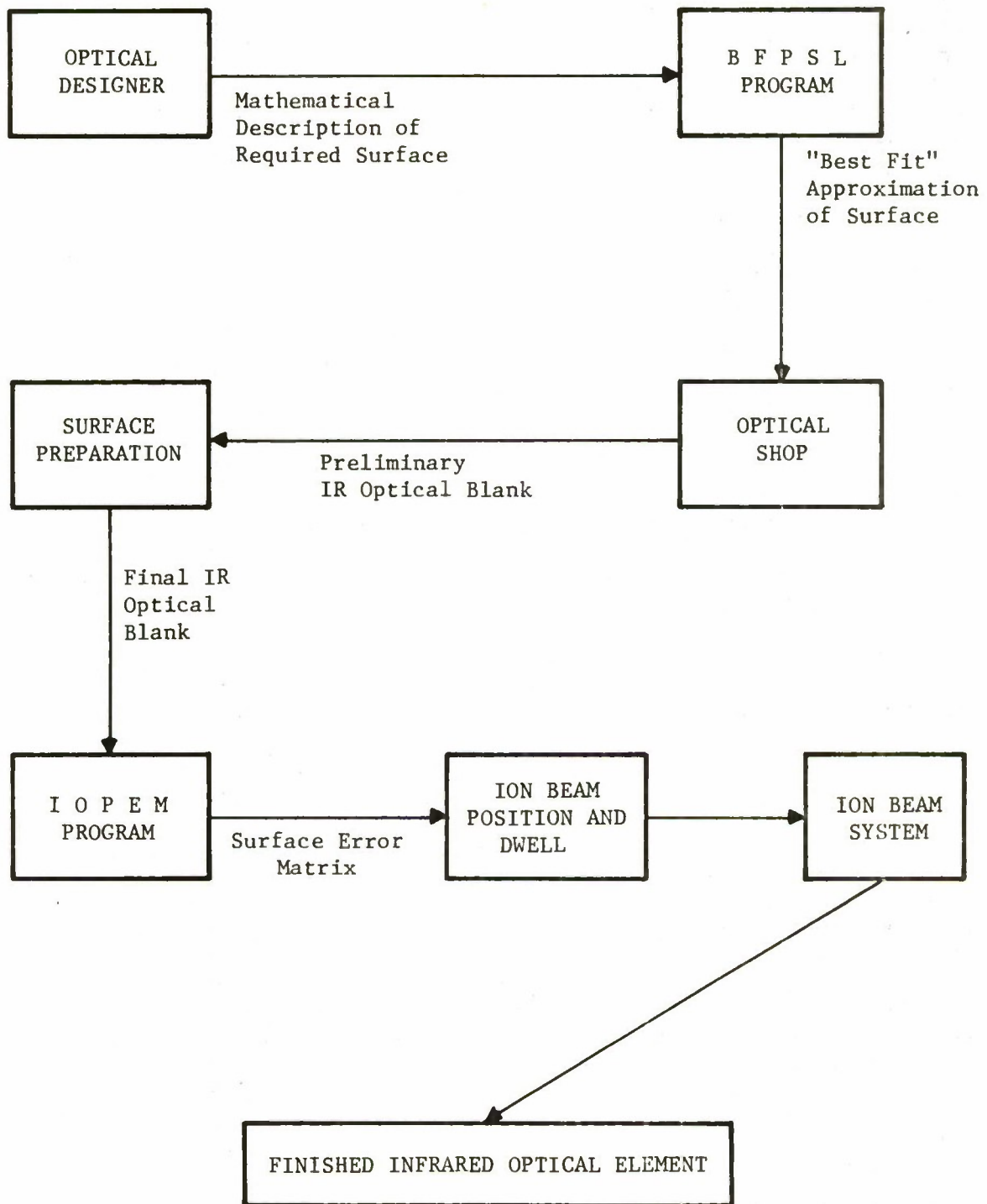


Figure 12. IR Optical Element Fabrication

Step 6 - The prepared infrared optical blank is shaped by an ion beam, under the control of the dedicated mini computer. This process takes place in a vacuum better than 10^{-6} torr. Because of the precision, the process proceeds directly to the final desired surface without any further surface contour measurements.

SYSTEM HARDWARE

The positive ion accelerator utilized by Frankford Arsenal was designed specifically by Accelerators Inc., Austin, Texas for optical polishing. Figure 13 is a diagram of the accelerator, and a photograph is shown in Figure 14. The accelerator is a linear device with a radio frequency (RF) source capable of producing well defined and precisely focused beams of ions of various species. The system is capable of producing a 0 to 50 KeV beam of singly ionized Argon (Ar^+) with currents as high as 1.5 milli-amperes within a 5-mm beam diameter at the target. The system has a dual axis electrostatic deflection system which is capable of ± 10 centimeters deflection in both orthogonal axes at the target surface.

The deflection system is driven by fast response, DC coupled voltage amplifiers which are controlled by the outputs of two independent D-A voltage sources. A Hewlett-Packard 2116A minicomputer drives the D-A voltage sources. Several faraday cups are located in the target plane. The output of these faraday cups is sampled by the minicomputer at operator specified intervals through an A-D interface. The minicomputer is directly interfaced to a 9-track digital magnetic tape recorder which is used for storage of large quantities of surface error matrix data.

CONCLUSIONS

All the data necessary for the establishment of a facility capable of fabricating infrared optical elements using a computer controlled ion beam has been established. The complex interactions which result in undesired surface decorations have been described together with a description of instrumentation capable of providing an accurate quantitative measurement of surface defects. A practical method of fabricating high quality, uncontaminated infrared optical elements has been developed. This information will be applied under a follow-on project which will result in the implementation of the data presented in this report by establishing a facility for producing infrared optical elements.

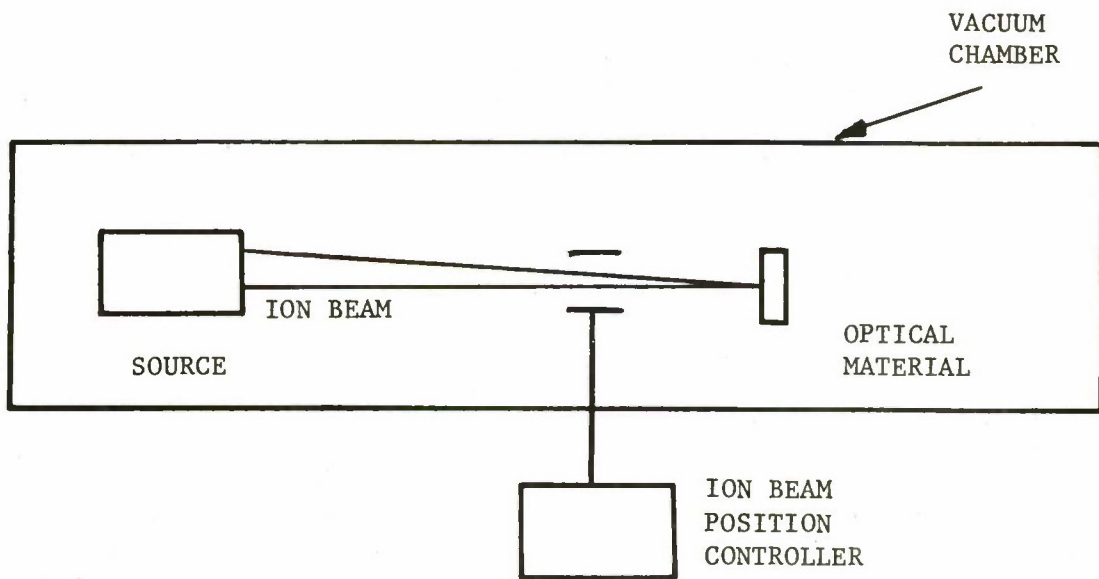


Figure 13. Schematic, Low Energy Ion Beam Accelerator

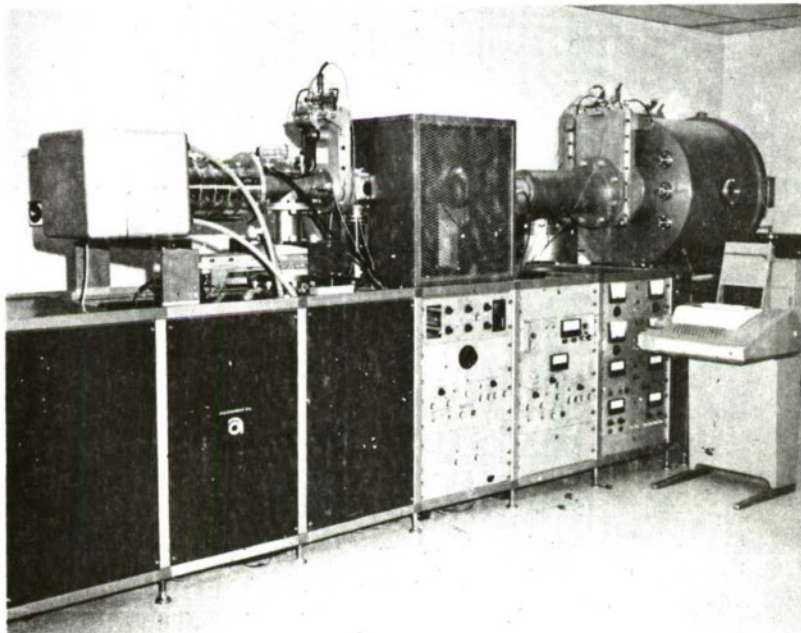


Figure 14. Low Energy Ion Beam Accelerator

REFERENCES

1. J. D. Lester, Forming Precision Optics Using an Ion Beam, Frankford Arsenal Report R-2087, (1973).
2. G. D. Magnuson, B. Meckel and P. Harkins, J. Appl. Phys. 32, 369 (1961).
3. R. Cunningham et al, J. Appl. Phys. 31, 839 (1960).
4. G. Wehner, Phys. Rev. 102, 690 (1956).
5. E. Lamar and K. Compton, Science 80, 541 (1934).
6. D. T. Goldman and A. Simon, Phys. Rev. 111, 383 (1958).
7. E. Henschke, Phys. Rev. 121, 1286 (1961).
8. E. Langberg, Thesis Dept. Elect. Eng., Princeton Univ. (1956).
9. P. Rol. J. Fluit and J. Kistemaker, Physica 26, 1009 (1960).
10. Yu. V. Martynenko, Soviet Phys. Sol. State 6, 1581 (1965).
11. Yu. V. Martynenko, Soviet Phys. Sol. State 6, 2827 (1965).
12. G. Carter and J. Colligon, Ion Bombardment of Solids, New York, American Elsevier Publishing Company, 1968.
13. H. E. Bennett and J. O. Porteus, J. Opt. Sol. Am, 51, 123 (1961).
14. W. B. Ribbens, Appl. Optics 8, 2173 (1969).
15. J. Motycka, Appl. Optics 8, 1435 (1969).
16. B. Hildebrand, "Surface Roughness Measurements by an Optical Heterodyne Technique", IMOG Subgroup on Gaging, 33rd Meeting (1972).
17. J. M. Bennett, J. Opt. Soc. Am. 54, 612 (1964)
18. R. W. Dietz and J. M. Bennett, Appl. Optics 5, 81 (1966).
19. B. Hildebrand, R. Gordon and E. Allen, Appl. Optics 13, 177 (1974).
20. Reported in: Microinch Machining of Optical Components for Infrared Optics by Capt. T. T. Saito, USAF, Air Force Weapons Laboratories, Rept. AFWL-TR-73-290 (1974).
21. L. Maissel and R. Glang, Handbook of Thin Film Technology, McGraw-Hill, NY, NY (1970).

REFERENCES (Cont'd)

22. E. Bernal et al, Preparation and Characterization of Polycrystalline Halides for Use in High Power Laser Windows, Honeywell Research Center, Rept. No. HR-74-252:5-26 ARPA Order Nos. A02172/1 and AD2416 (1974).
23. L. Maissel, Loc Cit.
24. G. Bassett Proc. European Conf. Electron Microscopy. DELFT (1960).
25. J. D. Lester and R. T. Cook, Ion Beam Superpolishing of Metal Mirrors, Proc. 1974 Frankford Arsenal Spring Technical Symposium (1974).
26. M. J. Soileau et al in High Energy Laser Mirrors and Windows, H. Bennett, editor Semi-annual report No. 4 ARPA Order 2175 (1974).

DISTRIBUTION

Commander
US Army Materiel Development
and Readiness Command
5001 Eisenhower Ave.
Alexandria, VA 22203

1 Attn: DRCDE-R

1 Attn: DRC-PP

Director
US Army Production Equip Agency
Attn: AMXPE-MT
Mr. C. McBurney
Rock Island, IL 61201

Commander
US Army Armament Command
Rock Island, IL 71202

1 Attn: DRSAR-PPP

1 Attn: DRSAR-RDT

1 Attn: DRSAR-ASF

1 Attn: DRSAR-RDR

1 Attn: DRSAR-MA (Bldg. 30)

Commander
Picatinny Arsenal
2 Attn: Scientific & Technical
Information Branch
Dover, NJ 07801

US Army Field Office
HQ AFSC/SDOA
Andrews AFB, DC 20334

Department of the Navy
USA Mobility Equipment
Research & Development Center
Attn: AMXFB-DS
Ft. Belvoir, VA 22060

US Army Electronics Command
Attn: Dr. Rudolf G. Buser,
AMSEL-CT-L
Ft. Monmouth, NJ 07703

Michelson Lab.
Naval Weapons Center
Attn: H. E. Bennett, Code 6018
China Lake, CA 93555

Commander
US Army Missile Command
Attn: AMSMI-IDD
Redstone Arsenal, IL

Commander
US Army Aviation Materiel Command
P.O. Box 209, Main Office
Attn: AMSAV-MN
St. Louis, MO 63166

Commander
Bolling Air Force Base
Attn: Mr. J. Cahill
Washington, DC

Commander
Naval Air Development Center
Attn: Mr. J. Parker
Johnsville, PA 18974

Commander
Rome Air Development Center
Attn: RADC (EMEDE)
Griffiss AFB, NY 13440

Commander
US Air Force Avionics Laboratory
Attn: Mr. Steinbergen -AVTA
Wright Patterson AFB, OH

Commander
US Naval Research Laboratory
Washington, DC 20390

1 Attn: Mr. J. P. Gumn

1 Attn: Mr. C. M. Herbert

Commander
Attn: SAAMA (SANSS)
Kelly AFB, TX 78241

DISTRIBUTION (Cont'd)

Accelerators Incorporated
Attn: Pieter M. De Bruijn
212 Industrial Blvd.
Box 3293
Austin, TX 78764

Defense Documentation Center (12)
Cameron Station
Alexandria, VA 22314

Commander
Frankford Arsenal
Phila., PA 19137

1 Attn: SARFA-AOA-M/107-B

1 Attn: SARFA-TD/107-1

1 Attn: SARFA-PA/107-2

1 Attn: SARFA-QAA-R/119-2

1 Attn: SARFA-GC/40-1

1 Attn: SARFA-FCD-M/201-3

1 Attn: SARFA-MTT-O/110-3
Project File

1 Attn: SARFA-MTT-O/110-3
Chf, Optics & Electronics

8 Attn: SARFA-FCD-M/201-3
J. Lester

1 Attn: SARFA-MTT/211-2

1 Attn: SARFA-MT/211-2

1 Attn: SARFA-FCD/201-3
Chief, System Dev. Div.

3 Attn: SARFA-TSP-L/51-2
(1 - Circulation copy
1 - Reference copy
1 - Record copy)

Printing & Reproduction Division
FRANKFORD ARSENAL

Date Printed: 27 April 1976